ORNL/CP98633

CONF-980645--

MODELING OF NUCLEATION DURING RECRYSTALLIZATION

B. Radhakrishnan, G. Sarma and T. Zacharia

Oak Ridge National Laboratory
P.O. Box 2008, MS-6140
Oak Ridge, TN 37831-6140, USA

Abstract

The number density and spatial distribution of nuclei determine the kinetics, and the evolution of microstructure and texture during recrystallization. The potential nucleation sites are the high angle boundaries that exist in the deformed microstructure. These could be either the original grain boundaries prior to deformation or boundaries created due to non- uniform plastic deformation on the microscopic scale. Discontinuous subgrain growth with or without the formation of high angle boundaries may also occur during recrystallization in the presence of long range orientation gradients existing in the deformation substructure. The paper presents Monte Carlo simulation results on the evolution of substructures for each of the above nucleation mechanisms. The evolution of recrystallized grain structure from a realistic substructure obtained by modeling the deformation of fcc polycrystals at the microstructural level is presented, and shows the collective contribution of the above nucleation mechanisms during recrystallization and grain growth. The simulations capture not only the kinetics and microstructural evolution but also the evolution of texture during recrystallization.

Introduction

Recrystallization has traditionally been represented as a two-step process involving distinct nucleation and growth stages, similar to the classic diffusional phase transformations. This is because of the general observation that recrystallization is characterized by the presence of an incubation phase during which many locations in the deformed microstructure "nucleate" strain-free grains generally bounded by high-angle boundaries, followed by a growth phase in which these boundaries sweep through the deformed microstructure. However, it is known that the mechanism of nucleation during recrystallization is different from that in phase transformations. With a driving force that is much smaller than that for phase transformations, and a large surface energy of the grain boundaries, the critical nucleus size for recrystallization is of the order of a micron, which cannot be obtained by atomic fluctuations as in phase transformations [1].

The detailed observations of dislocation substructures in cold worked materials using the recently developed microtexture measurement technique based on Electron Back Scattering Pattern (EBSP) analysis in the transmission electron microscope (TEM) have clearly revealed the formation of high-angle boundaries by grain subdivision mechanisms [2]. These high angle boundaries are called "geometrically necessary boundaries" because the formation of such boundaries is required to separate regions of a single prior grain that have rotated to vastly different final orientations during deformation due to the operation of different sets of slip systems. Within the highly misoriented regions, the substructure consists of cells or subgrains of low misorientations. By using the EBSP technique in a Scanning Electron Microscope (SEM), it was also possible to detect long range orientation gradients in the deformed substructure of commercial purity aluminum both along the rolling and transverse directions [3]. It is now known that substructural features are the potential nucleation sites for recrystallization.

The number density and the spatial distribution of nuclei play an important role in the development of the recrystallized microstructure and texture. Non-randomness in the distribution of nuclei leads to early impingement of recrystallization fronts, and a reduction in recrystallization rate due to decreased dimensionality of growth. Texture components that nucleate randomly have a greater potential for uninterrupted growth, and hence may dominate the recrystallization texture.

The spatial distribution of nuclei also determines the grain size distribution that results from recrystallization. Nuclei of high angle boundaries which impinge very early in the growth stage will result in small grains while those that grow uninterrupted will produce large grains. The discontinuous growth of subgrains due to orientation gradients may also produce large grains with boundary misorientations that depend on the orientation gradient. Finally, those regions of the microstructure which are not swept by discontinuous growth will evolve through uniform recovery by subgrain growth, and will generally be present as "recovered" regions with a small mean grain size. The grain size distribution after recrystallization will depend upon the relative contributions of the above growth components and will depend strongly on the deformation substructure. The ability to accurately capture the grain size distribution after recrystallization is an important measure of success of any modeling effort in this area.

The spatial distribution of nucleation sites depends upon the substructure produced by deformation. Hence, in order to realistically capture the kinetic, microstructural and textural effects during recrystallization, it is necessary to develop recrystallization models which are closely coupled to microstructural deformation models that can provide a quan-

titative description of the cold worked state. One such model has recently been developed by coupling a finite element (FE) simulation of microstructural deformation based on crystal plasticity with a Monte Carlo (MC) simulation of subgrain growth [4].

The objectives of this paper are to simulate, (i) discontinuous growth triggered by individual substructural features such as deformation induced high-angle boundary and subgrain orientation gradient described above, (ii) the effect of the above substructural parameters on the growth kinetics, and (iii) the combined operation of several such discontinuous growth fronts during the recrystallization of a realistic deformation substructure through the coupled FE-MC model [4]. The simulations are used to illustrate the effect of prior deformation on the recrystallization kinetics, texture, grain size and grain size distribution.

Computational Approach

The MC technique [4] is used for simulating the discontinuous growth of a deformation induced high angle boundary embedded in a subgrain network or the discontinuous growth of subgrains induced by an orientation gradient [4]. In this technique, a subgrain network containing one of the above features is mapped to a regular grid of points. Each grid point represents material with a certain crystallographic orientation. Points which have the same crystallographic orientation belong to the same grain. The grain boundaries are not modeled explicitely. A grain boundary is assumed to exist between two points with different orientations.

Each site is visited in a random fashion and the local energy of the site and its neighborhood, E_{init}, is calculated using

$$E_{init} = \sum_i \gamma_i, \tag{1}$$

where γ_i is the specific boundary energy between the site and its i^{th} neighbor. γ_i is a function of the misorientation between the two sites and it is given by

$$\gamma = \begin{cases} \gamma_m \frac{\theta}{\theta^*}\left[1 - \ln\left(\frac{\theta}{\theta^*}\right)\right] & \text{when } \theta \leq \theta^*, \\ \gamma_m & \text{when } \theta > \theta^*, \end{cases} \tag{2}$$

where θ is the misorientation between the two sites, γ_m is the energy per unit area of a high-angle boundary, and θ^* is the misorientation limit for low angle boundaries, which is usually taken as 15°. The energy of the site and its neighborhood when its orientation is replaced by the orientation of one of its nearest neighbors, E_{fin}, is then calculated as

$$E_{fin} = \sum_i \gamma_i', \tag{3}$$

where γ_i' is the misorientation dependent specific boundary energy between the replaced neighboring orientation and the original neighborhood of the site. The local energy change ΔE is calculated as $E_{fin} - E_{init}$. The probability of flipping the site to the orientation of the chosen nearest neighbor, p, is calculated as

$$p = \begin{cases} k' & \Delta E \leq 0 \\ k' \exp(-\Delta E/kT) & \Delta E > 0 \end{cases} \tag{4}$$

where k is Boltzmann's constant and k' is the misorientation-dependent boundary mobility given by [5]

$$k' = \left[1 - \exp(-q\theta^3)\right], \tag{5}$$

where q is a constant, assumed to be 0.001 in the current simulations. In equation (4), T is not the absolute temperature. It is the lattice temperature, which, in MC simulations, is related to the critical lattice temperature at which the domain becomes fully disordered. In the current simulations, the quantity kT was assumed to be 0.4 times the energy of a high angle boundary. The reorientation of the site is implemented with the probability p calculated using equations (4) and (5).

The formation of a realistic deformation substructure that contains several potential discontinuous growth fronts, and the combined operation of these growth fronts are simulated by using a coupled FE-MC approach. In this approach, the deformation microstructure is first obtained by using the FE simulation [6]. The initial microstructure is discretized such that there are several hundred elements per grain. The unique feature of the FE simulations is that it captures the heterogeneity of deformation at the scale of the microstructure and provides a quantitative description of the stored energy, plastic strain and crystallographic orientation distributions in the deformed microstructure.

In order to utilize the above microstructural information in the recrystallization model, it has to be first mapped from a deformed FE mesh to a regular grid. The mapping is carried out using a procedure described elsewhere [6]. The deformation substructure at each grid point is then obtained from a knowledge of the stored energy per unit volume at the site. Each site is assumed to consist of a subgrain network with a mean subgrain size and a mean subgrain misorientation. The stored energy per unit volume at a site, H, is assumed to be the energy per unit volume of the subgrain network given by,

$$H = \frac{2\gamma}{D}, \tag{6}$$

where D is the mean subgrain size and γ is the energy per unit area of a subgrain boundary given by equation (2). Equations (2) and (6) are used to calculate the mean misorientation between subgrains at every site, assuming that the mean subgrain size at each site is 1/15 the site size. The calculations result in a local sublattice for each site in the form of a subgrain network with a known subgrain size and misorientation between the subgrains. These sublattices are assembled to generate a global lattice that contains the deformation substructure for the entire volume. The MC simulation technique described above is then used to simulate the discontinuous evolution of the substructure during annealing.

Simulations

As described previously, two different sets of MC simulations were carried out in this study. The objective of the first set of simulations was to illustrate discontinous evolution of a substructure due to the individual presence of (a) a high angle boundary, and (b) an orientation gradient in the substructure, and the influence of substructure parameters on the kinetics of discontinuous evolution. The objective of the second set of simulations was to study the effect of the simultaneous operation of many high angle boundaries and orientation gradients in a realistic deformation substructure.

The first set of simulations was carried out in a 200 $\times$ 200 triangular lattice. Each lattice site was characterized by a distinct orientation number. The misorientation between the subgrains in the lattice was 2.0°. A circular region of a given diameter centered at (100,100), the center of the simulation domain, was introduced and an orientation number of 50° was assigned to these sites. The mean subgrain size and the mean subgrain misorientation in the inner region were varied such that the inner region had either a lower or higher subgrain boundary energy per unit area than the outer region.

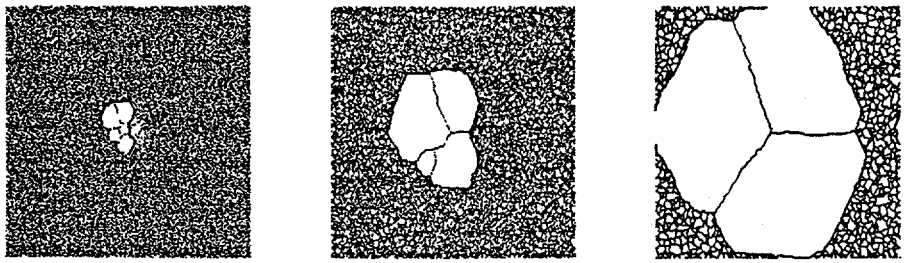

Figure 1: Temporal evolution of subgrain structure containing low energy and high energy regions separated by a high angle boundary.

The discontinuous movement of the high angle boundary segments between the inner and outer regions occurred due to the stored energy difference between the two regions, as given by equations (6) and (2). The discontinuous growth of subgrains in an orientation gradient was simulated by varying the orientation between the subgrains as a function of the radial distance from the center of the simulation domain in a linear fashion. The width and peak of the orientation distribution were the key variables considered in these simulations.

The second set of simulations was carried out by using an initial substructure obtained by microstructural deformation modeling described previously. The deformation modeling was carried out using a realistic three-dimensional grain structure for an fcc material under plane strain compresssions to 50% or 68% reduction in height. The deformation volume in each case was then mapped to a $30 \times 30 \times 30$ cubic lattice. Sections of the three-dimensional deformed microstructure were used in two-dimensional MC simulations of substructure evolution. The substructure at each site of the 30×30 grid was modeled using a 15×15 sublattice, with a subgrain size of one sublattice site, leading to a global sublattice size of 450×450. The mean subgrain misorientation at each site was calculated as described previously, using equations (2) and (6). A neighborhood consisting of the 4 first-nearest neighbors and the 4 second-nearest neighbors was used for the local energy calculations in equations (1) and (3).

Results and Discussion

Fig. 1 shows the temporal evolution of the high angle boundary when the stored energy of the substructure inside the central region is lower than that outside. The lower stored energy in the central region of Fig. 1 was obtained by decreasing the mean misorientation between subgrains for the same mean subgrain size. The discontinuous outward migration of the high angle boundary results in the formation of a large grain at the center, essentially free of substructure except for the three low angle boundaries. The character of the initial high angle boundary also changes at some locations resulting in the formation of low angle boundary segments. The high and low angle boundaries in Fig. 1 as well as in the subsequent figures are shown by thick and thin lines, respectively. The recrystalization kinetics, as measured by the fractional area of the discontinuously growing front as a function of simulation time in Monte Carlo steps (MCS), is shown in Fig. 2. The recrystallization rate in this case is seen to increase with decreasing subgrain misorientation as shown in Fig. 2(a), which corresponds to increasing driving force. A similar outward migration of the high angle boundary was observed with the formation of high and low

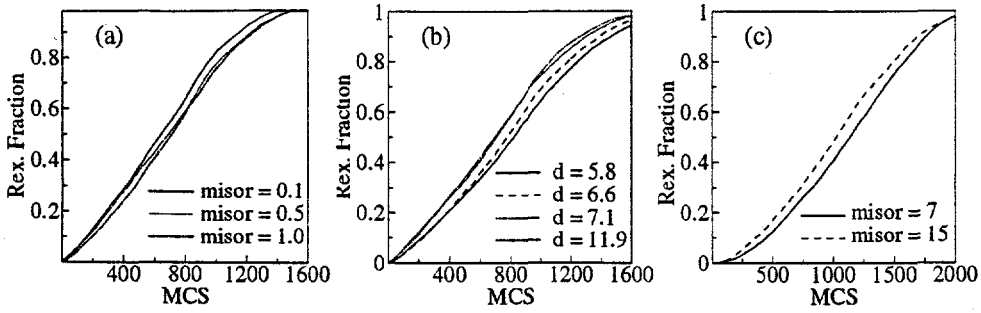

Figure 2: Recrystallization kinetics corresponding to cases where the lower stored energy in the central region is obtained by (a) lower subgrain misorientation and (b) larger subgrain size. In (c) the initial stored energy in the central region is higher because of higher subgrain misorientation than outside. In all cases, the inner and outer regions are separated initially by a high angle boundary.

angle boundaries (see Fig. 1) when the initial lower energy in the central region was obtained by increasing the mean subgrain size for the same subgrain misorientation for the inner and outer regions. The recrystallization kinetics shown in Fig. 2(b) illustrates a similar relationship between recrystallization rate and driving force as in Fig. 2(a). In this case, the initial driving force increases with increasing initial subgrain size in the central region. Nucleation and growth resulting from low stored energy sites has been observed in experimental studies of recrystallization. The formation and growth of cube nuclei from deformed cube bands in Al alloys has been shown to occur by such a mechanism[7].

The nucleation mechanism described above can also operate when the initial stored energy in the central region is high compared to that in the outer region. This is because of the high rate of recovery by rapid subgrain growth in the central region, which ultimately results in a lower stored energy compared to that in the outer region. The rapid recovery is due to the small subgrain size and high subgrain misorientation associated with high stored energy. Fig. 2(c) shows that the recrystallization rate in this case increases with increasing initial subgrain misorientation in the central region, indicating the effect of recovery rate on the recrystallization rate. Such substructural features might exist in the deformation zones around hard particles where a highly deformed region adjacent to the hard particles may be surrounded by regions with lower levels of stored energy, resulting in particle stimulated nucleation (PSN).

An additional possibility that leads to discontinuous substructural evolution is the presence of long range orientation gradeints formed by inhomogeneous deformation at the microstructural level. Such long range orientation gradients, observed in transition bands, are also believed to be the cause of nucleation of cube orientations in Al alloys [8]. Fig. 3 shows the temporal evolution of substructure in the presence of an orientation gradient. The orientation profiles used in this study and the corresponding recrystallization kinetics are shown in Fig. 4. The orientation profiles were chosen such that a constant radial orientation gradient was imposed inside a central region of a given radius. Outside this region, the subgrains had a random misorientation. The orientation gradient and the region over which the gradient existed were the two variables studied. The temporal evolution of microstructure shown in Fig. 3 is in the presence of the orientation profile 4 shown in Fig. 4. Note the discontinuous evolution of the subgrains in the central region in the presence of the orientation gradient. The discontinuous growth results in the formation of a nucleus which has both high angle and low angle boundary segments, as shown in

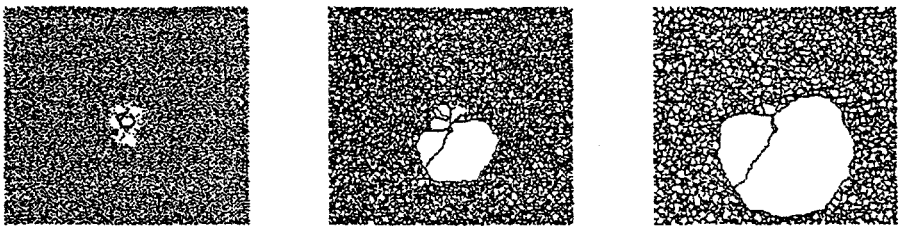

Figure 3: Temporal evolution of subgrain structure in the presence of an orientation gradient in the central region.

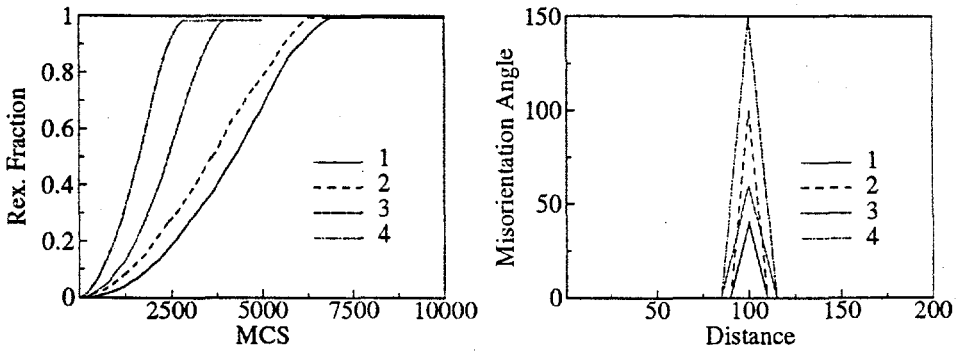

Figure 4: Orientation profiles used in this study.

Fig. 3(a). However, the high angle segment disappears after subsequent growth, as shown in Fig. 3(b). The fractional coverage of nuclei with high angle angle boundaries depends upon the local evolution of subgrains within the orientation gradient. A significant variation in the evolution of substructure was observed for the same initial microstructure and orientation profile for different starting seed numbers used in the random number generator. This is because the region within which the discontinuous evolution occurs is small and not statistically significant. However, it can be seen from Fig. 4 that the recrystallization kinetics increases with the radial distance over which orientation gradient exists as well as with the misorientation between subgrains (which depends upon the magnitude of the orientation gradient).

The above simulations indicate that the presence of substructural features of the type discussed above can trigger discontinuous evolution of the substructure. The deformation substructure typically consists of a spatial distribution of such features that are known to be a function of the amount of deformation, initial grain structure, the type of deformation, the crystal structure (number and type of slip systems), etc. Hence, it should be possible to simulate recrystallization as a discontinuous subgrain growth process, provided the deformation substructure is known quantitatively. Such a simulation would quantify the number density, the spatial distribution and the crystallographic orientations of the nucleating sites in the deformed substructure, and would provide a fundamental understanding of the evolution of microstructure and texture during recrystallization.

Fig. 5 shows the temporal evolution of the deformation substructure of an fcc polycrystal corresponding to plane strain compression of 50%. Note that the high angle boundaries present in the deformation substructure migrate in a discontinuous fashion, resulting in recrystallization. A detailed examination of the initial and deformed microstructures in-

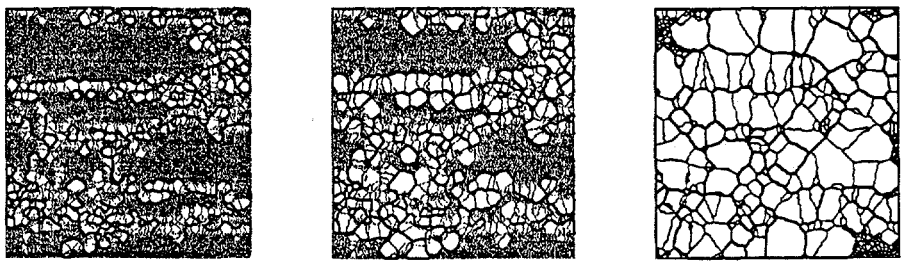

Figure 5: Temporal evolution of deformation substructure in a polycrystalline material obtained by coupled FE-MC simulation.

dicates that some of the high angle boundaries have been produced by the deformation process. Discontinuous growth of the substructure is also observed in locations free of high angle boundaries, probably due to the presence of orientation gradients introduced by deformation. The simulations also capture the influence of the extent of prior deformation on the recrystallization kinetics, as shown in Fig. 6. The higher initial deformation results in a more random distribution of the nucleation sites of the types described above, leading to more complete recrystallization. The deviation from ideal Johnson-Mehl-Avrami-Kolmogorov kinetics due to non-random nuclei distribution and non-isotropic growth is also shown in Fig. 6. Higher amount of initial deformation also leads to the expected finer recrystallized grain size as shown in Fig. 7.

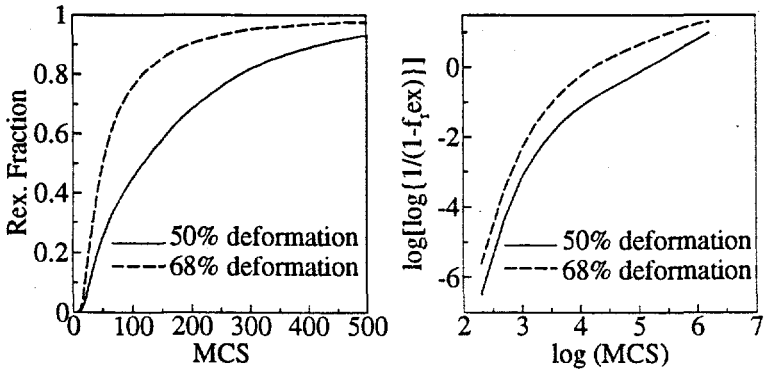

Figure 6: Effect of amount of prior deformation on recrystallization kinetics.

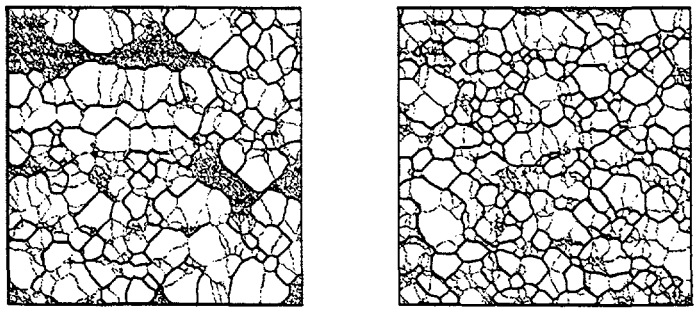

Figure 7: Effect of amount of prior deformation on recrystallized grain size.

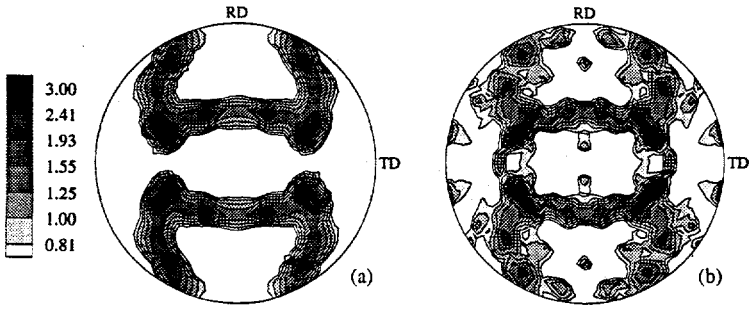

Figure 8: (a) Deformation and (b) recrystallization textures showing the formation near cube orientations after recrystallization.

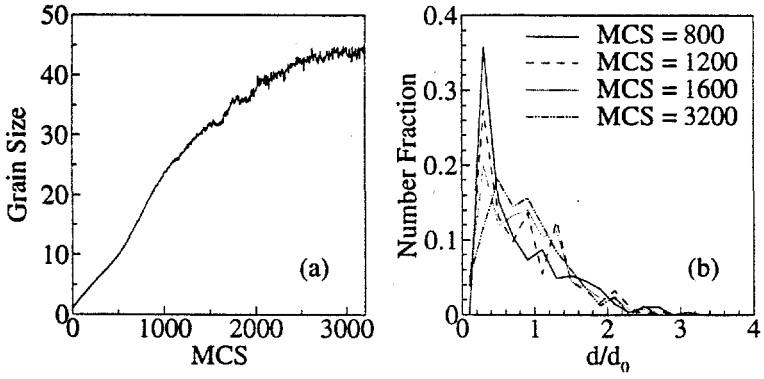

Figure 9: Evolution of (a) grain size and (b) grain size distribution as a function of annealing time.

In the above MC simulations, the orientation of each site is characterized by a complete description of the crystallographic orientation in terms of an axis-angle pair, which is provided by the deformation model. Hence, it is possible to monitor the evolution of crystallographic texture during recrystallization. A significant result obtained from these simulations is the evolution of cube texture during recrystallization of deformed fcc polycrystals shown in Fig. 8. Even though the deformation texture does not indicate the presence of cube orientations (no cube orientations were present prior to deformation), recrystallization causes some of the near cube orientations produced by deformation to grow due to the presence of locally favorable substructural features. The above mechanism of cube formation is similar to the one suggested by Dillamore and Katoh [8]. Simulation of cube formation from remnant cube orientations in the deformed grain structure is reported elsewhere [4].

Since the model treats recrystallization in the context of a subgrain growth process it provides a logical continuity between recrystallization and grain growth phenomena that occur simultaneously during annealing. The kinetics of subgrain growth during annealing is shown in Fig. 9. Note that the discontinuous subgrain growth associated with recrystallization results in an accelerated growth kinetics at early times, followed by a parabolic growth rate typical of grain growth after the recrystallization process is completed. The presence of "recovered" regions in the microstructure gives rise to a grain size distribution that is characterized by a large number of fine grains. With continued annealing, these regions ultimately disappear, giving rise to the typical grain size distribution observed in well-annealed materials.

Conclusions

The discontinuous migration of a high angle boundary present in a deformation substructure caused by a difference in the stored energy of deformation across the boundary, and and the discontinuous subgrain growth due to long-range orientation gradients are illustrated through MC simulations. The evolution of a realistic deformation substructure by the combined operation of such discontinuous growth mechanisms capture not only the kinetic and microstructural features of recrystallization and grain growth, but also the evolution of recrystallization texture because of the ability to capture the orientations of the potential nucleation sites.

Acknowledgments

This research was sponsored by the Office of Basic Energy Sciences, U.S. Department of Energy, under contract DE-AC05-96OR22464 with Lockheed Martin Energy Research Corporation. The research was supported in part by an appointment to the Oak Ridge National Laboratory Postdoctoral Research Associates Program administered jointly with the Oak Ridge Institute for Science and Education. The authors acknowledge the use of the Intel Paragon XP/S 35 located in the Oak Ridge National Laboratory Center for Computational Sciences (CCS), funded by the Department of Energy's Office of Scientific Computing.

References

1. R.D. Doherty et al., Proc. of the 16th Risø Int. Symp. on Materials Science: Microstructural and Crystallographic Aspects of Recrystallization (Roskilde, Denmark: Risø National Laboratory, 1995), 1–23.

2. D.A. Hughes, "High Angle Boundaries Formed by Grain Subdivision Mechanisms," Acta. mater., 45 (1997), 3871–3886.

3. R. Ørsund, J. Hjelen and E. Nes, "Local Lattice Curvature and Deformation Heterogeneities in Heavily Deformed Aluminium," Scripta Metall., 23 (1989), 1193–1197.

4. B. Radhakrishnan, G. Sarma and B. Radhakrishnan, "Coupled Finite Element-Monte Carlo Simulation of Microstructure and Texture Evolution during Thermomechanical Processing," to be presented at Hot Deformation of Aluminum Alloys II, IL, Oct. 1998.

5. A.D. Rollett and E.A. Holm, Proc. ReX' 96, The Third Int. Conf. on Recrystallization and Related Phenomena (Monterey, CA: Monterey Institute of Advanced Studies, 1997), 31–41.

6. G. Sarma, B. Radhakrishnan and T. Zacharia, "Polycrystal Simulations of Texture Evolution during Deformation Processing," to be presented at Hot Deformation of Aluminum Alloys II, Rosemont, IL, October 1998.

7. H.E. Vatne et al. "Modeling Recrystallization after Hot Deformation of Aluminium," Acta. mater., 44 (1996), 4463–4473.

8. I. L. Dillamore and H. Katoh, "The Mechnisms of Recrystallization in Cubic Metals with Particular Reference to their Orientation-Dependence," Metal Science, 4 (1974), 73–83.